Glycoconjugate Journal 21, 377–386, 2004
© 2004 Kluwer Academic Publishers. Manufactured in The Netherlands.

Chemo-enzymatic synthesis and structure-activity study of artificially N-glycosylated eel calcitonin derivatives with a complex type oligosaccharide

Katsuji Haneda[1], Mizuka Tagashira[2], Eiichi Yoshino[1], Midori Takeuchi[1], Toshiyuki Inazu[1,3], Kazunori Toma[1], Hideki Iijima[2], Yukihiro Isogai[4], Masayuki Hori[4], Shinji Takamatsu[5], Yasuhisa Fujibayashi[5], Kazuo Kobayashi[6], Makoto Takeuchi[6] and Kenji Yamamoto[7]

[1] *The Noguchi Institute, 1-8-1, Kaga, Itabashi, Tokyo 173-0003, Japan,* [2] *Analytical Research Laboratory, Asahi Kasei Co., Fuji, Shizuoka 416-8501, Japan,* [3] *Department of Applied Chemistry, School of Engineering, Tokai Universtiy, Hiratsuka, Kanagawa 259-1292, Japan,* [4] *First Laboratory for Pharmacology, Asahi Kasei Co., Tagata, Shizuoka 410-2321, Japan,* [5] *High Energy Medical Research Center, Fukui Medical University, Yoshida, Fukui 910-1193, Japan,* [6] *Central Laboratories for Key Technology, Kirin Brewery Co., Kanazawa, Yokohama, Kanagawa 236-0004, Japan,* [7] *Graduate School of Biostudies, Kyoto University, Sakyo, Kyoto 606-8502, Japan*

Starting from N-glycosylated eel calcitonin derivatives that contain an *N*-acetyl-D-glucosamine residue specifically at the 3rd, 14th, 20th or 26th amino acid residue, corresponding glycopeptides with a complex-type oligosaccharide attached to the respective amino acid residue were synthesized by means of a transglycosylation reaction catalyzed by an endo-β-*N*-acetylglucosaminidase from *Mucor hiemalis*. The use of a recombinant enzyme and an excess of a glycosyl donor led to a yield in excess of 60%. Calcitonin derivatives containing truncated oligosaccharides were also prepared via digestion of the complex-type N-glycan with exoglycosidases. Using these N-glycosylated calcitonin derivatives, the effect of carbohydrate structure and glycosylation site on the three-dimensional structure and the biological activity of the peptide were studied. The conformation of the peptide backbone did not change irrespective of the carbohydrate structure or the glycosylation site. However, hypocalcemic activity, calcitonin-receptor binding activity and the biodistribution of the derivatives were affected by the glycosylation and were dependent on both the carbohydrate structure and the glycosylation site. Although the larger oligosaccharides tended to hinder receptor binding, the biodistribution altered by N-glycosylation appeared to enhance the hypocalcemic activity in some cases, and the magnitude of the effect was dependent on the site of glycosylation.
Published in 2004.

Keywords: **calcitonin, N-glycosylation, chemo-enzymatic synthesis, Endo-M, biological activity**

Abbreviations: **CT, calcitonin; CT-R, calcitonin receptor; GlcNAc, *N*-acetyl-D-glucosamine; Asn(GlcNAc), *N*-acetyl-D-glucosaminyl-L-asparagine; Gln(GlcNAc), *N*-acetyl-D-glucosaminyl-L-glutamine; NeuAc, *N*-acetyl-D-neuraminic acid; Gal, D-galactose; Man, D-mannose; endo-M, endo-β-*N*-acetylglucosaminidase of *Mucor hiemalis*; SGP, sialyl glyco-hexapeptide derived from hen egg yolk, H-Lys-Val-Ala-Asn[(NeuAc-Gal-GlcNAc-Man)$_2$-Man-GlcNAc$_2$]-Lys-Thr-OH; STF, disialo biantennary complex-type oligosaccharide, (NeuAc-Gal-GlcNAc-Man)$_2$-Man-GlcNAc$_2$; ASTF, asialo biantennary complex-type oligosaccharide, (Gal-GlcNAc-Man)$_2$-Man-GlcNAc$_2$; dGal, (GlcNAc-Man)$_2$-Man-GlcNAc$_2$; Core, Man$_3$-GlcNAc$_2$; M$_1$GN$_2$, Man-GlcNAc$_2$; GN$_2$, GlcNAc$_2$; CT-XXX, CT derivative possessing XXX (oligo)saccharide; CTn-XXX, CT derivative containing the XXX (oligo)saccharide at the n-th position; TFA, trifluoroacetic acid; TFE, trifluoroethanol; MALDI-TOF MS, matrix-assisted laser desorption ionization time-of-flight mass spectrometry; CD, circular dichroism; NMR, nuclear magnetic resonance.**

To whom correspondence should be addressed: Dr. Katsuji Haneda, The Noguchi Institute, 1-8-1, Kaga, Itabashi, Tokyo 173-0003, Japan. Tel.: +81-3-5944-3212; Fax: +81-3-5944-3212; E-mail: BRA01375@nifty.ne.jp and Dr. Kazunori Toma, Tel.: +81-3-5944-3216; Fax: +81-3-5944-3216; E-mail: toma@noguchi.or.jp

Introduction

Oligosaccharides in glycoproteins have been shown to play important roles in numerous biological processes [1–4], but no systematic study has been reported on the effect of glycosylation

on the three-dimensional structure and biological activity of a peptide or protein. Our previous work involved studies of effects of glycosylation using eel calcitonin (CT) as a model peptide [5–10].

CT, a calcium metabolism-regulating peptide hormone, exhibits hypocalcemic activity. Both CT and synthetic derivatives thereof are used as therapeutic agents in the treatment of hypercalcemia, Paget's disease and osteoporosis [11]. CT has certain advantages as a model peptide, in that it assumes a helical three-dimensional structure in a hydrophobic environment and its extremely high activity permits the use of a small-dose in *in vivo* assays. Although the Asn3 residue of CT is a potential site for N-glycosylation and the Asn-Leu-Ser sequence is conserved among many species, CT is not glycosylated in its natural form. Therefore, it would be possible to study the effects of carbohydrates on the structure and the activity of a peptide via the use of glycosylated CT derivatives.

In previous studies, we have shown that high-mannose type oligosaccharides at Asn3 of CT had no effect on three-dimensional structure and modulated the biological activity rather mildly depending on the carbohydrate structure [5,6], but that O-glycosylation drastically affected both three-dimensional structure and biological activity depending on the glycosylation site [9,10]. In the present study, we report on an investigation of the effect of, not only the carbohydrate structure, but also the site of glycosylation of N-glycosylated CT derivatives on their three-dimensional structure and biological activity.

We developed a chemo-enzymatic method for the synthesis of a glycopeptide that combined both the chemical synthesis of a peptide possessing GlcNAc [12,13] and a transglycosylation reaction catalyzed by endo-β-*N*-acetylglucosaminidase [14,15]. We have successfully synthesized glycosylated CT derivatives that contained N-linked oligosaccharides at Asn3 by a transglycosylation reaction using endo-β-*N*-acetylglucosaminidase obtained from *Mucor hiemalis* (Endo-M) [16], with [Asn(GlcNAc)^3]-CT (CT3-GlcNAc) as a starting material, in which Asn3 was replaced by *N*-acetyl-D-glucosaminyl-L-asparagine (Asn(GlcNAc)) [17,18]. We also synthesized a CT derivative containing a high-mannose type oligosaccharide using an endo-β-*N*-acetylglucosaminidase obtained from *Arthrobacter protophormiae* (Endo-A) [19]. Transglycosylation catalyzed by an endo-glycosidase is one of the most powerful methods for the construction of glycopeptides, although a number of glycopeptide syntheses have been reported [20]. Since our report on the transglycosylation to CT, O'Connor *et al*. [21] and Ajisaka *et al*. [22] employed our method in glycopeptide syntheses.

To prepare a sufficient amount of N-glycosylated CT samples for the structure-activity study, we determined the conditions for obtaining optimum yields of glycosylated products. In the first part of this paper, we report on a synthetic method for preparing N-glycosylated CT derivatives. We examined the reaction conditions required to increase the yield of the transglycosylation product by Endo-M, and prepared more than ten mg of each derivative. We introduced complex-type N-linked oligosaccharides not only to the Asn residue but also to the Gln residue, where natural glycosylation never occurs.

In the second part, we examined how glycosylation affected the tertiary structure, the biological activity and the biodistribution of CT using the various synthesized N-glycosylated CT derivatives. The systematically synthesized N-glycosylated CT derivatives permitted the studies of both carbohydrate structure-dependent and glycosylation site-dependent effects.

Materials and methods

Other than specifically described in the following sections, commercially available materials were used, as received.

Starting materials

GlcNAc-peptides: The *N*-acetyl-D-glucosaminyl CT derivatives possessing GlcNAc at 3rd, 14th, 20th or 26th residue, [Asn(GlcNAc)^3]-CT (CT3-GlcNAc), [Gln(GlcNAc)^{14}]-CT (CT14-GlcNAc), [Gln(GlcNAc)^{20}]-CT (CT20-GlcNAc) or [Asn(GlcNAc)^{26}]-CT (CT26-GlcNAc), respectively, were prepared by and purchased from Peptide Institute Inc. (Osaka, Japan).

Endo-M: Purified recombinant Endo-M cloned in *Candida boidinii* [15,23] was used. The enzyme solution (in 20 mM phosphate buffer of pH 7.0 containing 0.15 M NaCl) showed 600 mU/ml of hydrolytic activity against a dansyl asialo biantennary complex-type glycosyl asparagine substrate at pH 6.0 and 37°C.

Glycosyl donor: As a glycosyl donor of a disialo biantennary complex-type oligosaccharide, a sialyl glyco-hexapeptide (SGP), H-Lys-Val-Ala-Asn[(NeuAc-Gal-GlcNAc-Man)$_2$-Man-GlcNAc$_2$]-Lys-Thr-OH, derived from hen egg yolk [24] was purchased from Taiyo Kagaku Co., Ltd. (Mie, Japan).

General procedure for the transglycosylation of disialo biantennary complex-type oligosaccharide

The reaction mixture (0.2 to 0.6 ml) consisted of 10 mM GlcNAc derivative of CT (glycoside acceptor), 100 mM SGP (glycosyl donor) and 120 mU/ml of Endo-M in 60 mM potassium phosphate buffer of pH 6.25. For the preparation of ten-mg scale samples, two or three batch reactions were performed. After incubation at 37°C for 20 min, the reaction was terminated by adding an equal volume of a cold aqueous solution of 0.5% trifluoroacetic acid (TFA), and the reaction mixture was analyzed by a reverse-phase (RP)-HPLC using a ϕ 4.6 × 250 mm ODS column (Mightysil RP-18; Kanto Kagaku, Tokyo, Japan). The column was eluted with a linear increase in acetonitrile concentration in a 0.1% TFA aqueous solution over 40 min at a flow rate of 0.8 ml/min. The absorbance of the elution was monitored at 214 nm. The transglycosylation yield (mol %) was calculated from the ratio of the peak area corresponding

to the transglycosylation product to the initial peak area of the acceptor without consideration of the remaining acceptor. The calculation was based on the assumption that the molar absorption coefficient of the transglycosylation product was equal to that of the glycoside acceptor. The transglycosylation product was isolated by preparative RP-HPLC (ϕ 20 × 250 mm column), and then freeze dried. The structure of the product was confirmed by matrix-assisted laser desorption ionization time-of-flight mass spectrometry (MALDI-TOF MS) in the positive ion mode using α-cyano-4-hydroxycinnamic acid as a matrix on a Voyager Biospecrtometry Workstation (PerSeptive Biosystems, Framingham, MA).

[Asn{(NeuAc-Gal-GlcNAc-Man)$_2$-Man-GlcNAc$_2$}^{3}]-CT (CT3-STF): From 33.3 mg of CT3-GlcNAc, 23.6 mg of CT3-STF was obtained (46%; isolation yield without the consideration of the recovered acceptor). Transglycosylation yield: 58%. RP-HPLC: 28.2 min (27.5 to 37.5% acetonitrile). MALDI-TOF MS: found m/z $[M+H]^+$ 5624.5, calcd. for $C_{230}H_{377}N_{49}O_{108}S_2$ $[M+H]^+$ 5621.9.

[Gln{(NeuAc-Gal-GlcNAc-Man)$_2$-Man-GlcNAc$_2$}^{14}]-CT (CT14-STF): From 43.0 mg of CT14-GlcNAc, 24.3 mg of CT14-STF was obtained (36%). Transglycosylation yield: 60%. RP-HPLC: 24.9 min (30 to 40% acetonitrile). MALDI-TOF MS: found m/z $[M+H]^+$ 5621.1, calcd. for $C_{230}H_{377}N_{49}O_{108}S_2$. $[M+H]^+$ 5621.9.

[Gln{(NeuAc-Gal-GlcNAc-Man)$_2$-Man-GlcNAc$_2$}^{20}]-CT (CT20-STF): From 25.5 mg of CT20-GlcNAc, 15.8 mg of CT20-STF was obtained (40%). Transglycosylation yield: 62%. RP-HPLC: 17.3 min (30 to 37.5% acetonitrile). MALDI-TOF MS: found m/z $[M+H]^+$ 5621.0, calcd. for $C_{230}H_{377}N_{49}O_{108}S_2$. $[M+H]^+$ 5621.9.

[Asn{(NeuAc-Gal-GlcNAc-Man)$_2$-Man-GlcNAc$_2$}^{26}]-CT (CT26-STF): From 25.6 mg of CT26-GlcNAc, 19.4 mg of CT26-STF was obtained (49%). Transglycosylation yield: 67%. RP-HPLC: 30.9 min (30 to 35% acetonitrile). MALDI-TOF MS: found m/z $[M+H]^+$ 5620.8, calcd. for $C_{230}H_{378}N_{50}O_{107}S_2$ $[M+H]^+$ 5620.9.

General procedure for neuraminidase treatment

CT derivatives containing an asialo complex-type oligosaccharide (CT-ASTF) were prepared by treatment of the corresponding CT derivatives containing disialo biantennary complex-type oligosaccharides (CT-STF) with neuraminidase. The reaction mixture consisted of 1 mM CT-STF and 0.5 U/ml of *Arthrobacter ureafaciens* neuraminidase (Nacalai Tesque, Kyoto, Japan) in 60 mM acetate buffer of pH 5.0, and was incubated at 37°C for 40 to 90 min. The de-sialylated product was isolated by RP-HPLC.

[Asn{(Gal-GlcNAc-Man)$_2$-Man-GlcNAc$_2$}^{3}]-CT (CT3-ASTF): From 17.87 mg of CT3-STF, 14.54 mg of CT3-ASTF was obtained (91%). RP-HPLC: 29.2 min (27.5 to 37.5% acetonitrile in 0.1% TFA aq. over 40 min). MALDI-TOF MS: found m/z $[M+H]^+$ 5037.9, calcd. for $C_{208}H_{343}N_{47}O_{92}S_2$ $[M+H]^+$ 5039.4.

[Gln{(Gal-GlcNAc-Man)$_2$-Man-GlcNAc$_2$}^{14}]-CT (CT14-ASTF): From 9.00 mg of CT14-STF, 6.79 mg of CT14-ASTF was obtained (84%). RP-HPLC: 25.1 min (30 to 35% acetonitrile in 0.1% TFA aq. over 40 min). MALDI-TOF MS: found m/z $[M+H]^+$ 5039.6, calcd. for $C_{208}H_{343}N_{47}O_{92}S_2$ $[M+H]^+$ 5039.4.

[Gln{(Gal-GlcNAc-Man)$_2$-Man-GlcNAc$_2$}^{20}]-CT (CT20-ASTF): From 8.48 mg of CT20-STF, 4.80 mg of CT20-ASTF was obtained (65%). RP-HPLC: 24.5 min (28 to 31% acetonitrile in 0.1% TFA aq. over 40 min). MALDI-TOF MS: found m/z $[M+H]^+$ 5037.6, calcd. for $C_{208}H_{343}N_{47}O_{92}S_2$ $[M+H]^+$ 5039.4.

[Asn{(Gal-GlcNAc-Man)$_2$-Man-GlcNAc$_2$}^{26}]-CT (CT26-ASTF): From 7.54 mg of CT26-STF, 5.36 mg of CT26-ASTF was obtained (79%). RP-HPLC: 30.4 min (30 to 35% acetonitrile in 0.1% TFA aq. over 40 min). MALDI-TOF MS: found m/z $[M+H]^+$ 5038.9, calcd. for $C_{208}H_{344}N_{48}O_{91}S_2$ $[M+H]^+$ 5038.4.

[Asn{(GlcNAc-Man)$_2$-Man-GlcNAc$_2$}^{3}]-CT (CT3-dGal)

The reaction mixture consisted of 12.77 mg of CT3-ASTF, 10 U/ml of β-galactosidase from jack bean (Seikagaku Co., Tokyo, Japan) and 50 mM citrate buffer (pH 3.5) in a total volume of 500 μl, and was incubated at 37°C for 20 h. 10.99 mg of CT3-dGal was isolated (92%). RP-HPLC: 22.4 min (30 to 33% acetonitrile in 0.1% TFA aq. over 40 min). MALDI-TOF MS: found m/z $[M+H]^+$ 4717.9, calcd for $C_{196}H_{323}N_{47}O_{82}S_2$ $[M+H]^+$ 4715.1.

[Asn(Man$_3$-GlcNAc$_2$)^3]-CT (CT3-Core)

The reaction mixture consisted of 9.82 mg of CT3-dGal, 6.5 U/ml of β-*N*-acetylhexosaminidase from jack bean (Seikagaku Co., Tokyo, Japan) and 50mM citrate phosphate buffer (pH 5.0) in a total volume of 440 μl, and was incubated at 37°C for 2 h. 8.27 mg of CT3-Core was isolated (92%). RP-HPLC: 24.7 min (30 to 33% acetonitrile in 0.1% TFA aq. over 40 min). MALDI-TOF MS: found m/z $[M+H]^+$ 4309.0, calcd. for $C_{180}H_{297}N_{45}O_{72}S_2$ for $[M+H]^+$ 4308.7.

[Asn(Man-GlcNAc$_2$)^3]-CT (CT3-M$_1$GN$_2$)

The reaction mixture consisted of 7.02 mg of CT3-Core, 13 U/ml of α1-2,3,6-mannosidase from jack bean (Calbiochem, San Diego, CA) and 50mM acetate buffer (pH 4.5) containing 0.5 mM Zn^{2+} in a total volume of 400 μl, and was incubated at 37°C for 4 h. The two D-mannose residues were nearly completely (97%) removed, and 5.20 mg of CT3-M$_1$GN$_2$ was isolated (80%). RP-HPLC: 27.7 min (30 to 35% acetonitrile in 0.1% TFA aq. over 40 min). MALDI-TOF MS: found m/z $[M+H]^+$ 3986.1, calcd for $C_{168}H_{277}N_{45}O_{62}S_2$ $[M+H]^+$ 3984.5.

[Asn(GlcNAc$_2$)^3]-CT (CT3-GN$_2$)

The reaction mixture consisted of 3.00 mg of CT3-M$_1$GN$_2$, 3 U/ml of β-mannosidase from snail (Sigma Co., St. Louis, MO) and 50mM acetate buffer (pH 4.0) in a total volume of 150 μl, and was incubated at 37°C for 4 h. 2.43 mg of CT3-GN$_2$ was isolated (85%). RP-HPLC: 29.9 min (30 to 35% acetonitrile in 0.1% TFA aq. over 40 min). MALDI-TOF MS: found m/z $[M+H]^+$ 3824.0, calcd. for $C_{162}H_{267}N_{45}O_{57}S_2$ $[M+H]^+$ 3822.3.

Circular dichroism (CD) measurement

CD spectra of the CT derivatives were obtained with a JASCO J-720 spectropolarimeter using aqueous solutions of 0, 10, 20, 40 or 60% trifluoroethanol (TFE) as previously reported [6]. The helical content was estimated according to the method of Chen *et al*. [25].

Hypocalcemic activity

The hypocalcemic activity of the CT derivatives was measured by a reported method [26]. A 0.2 ml aliquot of 1.8 (low dose) or 3.6 (high dose) pmol/ml sample solution was injected into the tail vein of male Sprague-Dawley rats, 4 to 5 weeks old, and the blood sample was taken 60 min after the injection. The serum concentration of calcium was determined with atomic absorption.

The blank value is the serum calcium concentration of the untreated animal, and the standard value is that of the animal injected with elcatonin, a synthetic analogue of eel CT [11]. 10 animals were sacrificed to determine the hypocalcemic activity at each low dose or high dose point. The standard deviation at each point was less than 5% in most of the cases as shown as raw data in a previous paper [6]. As the total result is a composite of several runs and the raw data is complicated, the low dose and high dose activity values of each CT derivative were averaged and are expressed relative (%) to that of CT in this report.

Receptor binding assay

The receptor binding activity of the CT derivatives was measured with a direct competition assay using mouse osteoclast-like cells and ^{125}I-labelled elcatonin [27,28] as described previously [6]. The IC_{50} value was obtained by fitting the raw data to the theoretical inhibition curve.

As the absolute value depends on the condition of osteoclast-like cells and the total result is a composite of three runs, we express the relative binding activity (%) of CT derivatives to that of CT in this report. The IC_{50} value and the corresponding 95% confidence limit in nM are as follows. Run 1: CT, 1.80 (1.17–2.78); CT3-GlcNAc, 2.10 (1.65–2.68); CT3-STF, 28.9 (15.8–53.1); CT3-ASTF, 8.69 (6.68–11.3); CT3-dGal, 4.63 (3.60–5.97); CT3-Core, 3.33 (2.84–3.92); CT3-M$_1$GN$_2$, 3.42 (2.58–4.53); CT3-GN$_2$, 2.33 (1.86–2.91); CT14-GlcNAc, 3.12 (2.23–4.36); CT14-STF, 65.9 (27.0–161); CT14-ASTF, 11.1 (6.29–19.5); CT20-GlcNAc, 1.74 (1.18–2.57); CT20-STF, 3.89 (3.18–4.76); CT20-ASTF, 2.72 (1.97–3.77). Run 2: CT, 0.948 (0.866–1.04); [Asn^{26}]-CT, 0.506 (0.437–0.587); CT26-GlcNAc, 0.444 (0.211–0.936). Run 3: CT, 2.03 (1.92–2.15); CT26-STF, 3.08 (2.32–4.08); CT26-ASTF, 1.89 (1.61–2.22).

Biodistribution

The biodistribution of the CT derivatives was determined using male ddY mice injected with ^{125}I-labelled samples as described previously [6]. The radioactivity in blood samples and organs of interest was measured, and tissue accumulation was calculated as a differential absorption ratio (DAR).

$$\mathrm{DAR} = 100 \times (\text{body weight} \times \text{sample count})/(\text{tissue weight} \times \text{injected count}).$$

Results

Synthesis of N-glycosylated CT derivatives

The N-glycosylated CT derivatives prepared in this study are listed in Table 1.

Although glycosyl asparagine prepared from human transferrin was used as a glycosyl donor of a complex-type oligosaccharide in our previous study [18], we employed SGP prepared from hen egg yolk [24], H-Lys-Val-Ala-Asn[(NeuAc-Gal-GlcNAc-Man)$_2$-Man-GlcNAc$_2$]-Lys-Thr-OH, as a glycosyl donor of the disialo biantennary complex-type oligosaccharide in this study. In addition, recombinant Endo-M [15,23] was employed in this study instead of the native enzyme prepared from *M. hiemalis*.

Using CT3-GlcNAc as a glycoside acceptor, we examined the transglycosylation reaction from SGP to an acceptor. The reaction mixture consisted of 10 mM of CT3-GlcNAc, 25 to 100 mM SGP and 120 mU/ml of Endo-M in 60 mM potassium phosphate buffer of pH 6.25. After a 20 min incubation at 37°C, the reaction mixture was analyzed by RP-HPLC. Figure 1 shows the effect of glycosyl donor concentration on the transglycosylation reaction. Transglycosylation from SGP to CT3-GlcNAc proceeded efficiently (Figure 1a). The use of an excess of the SGP glycosyl donor promoted the reaction in a dose dependent manner. The transglycosylation yield exceeded 50% at SGP concentrations of 75 to 100 mM. The transglycosylation of CT26-GlcNAc also proceeded with a similar efficiency, and the HPLC yield exceeded 60%, as shown in Figure 1b.

For the introduction of the N-linked oligosaccharide at either Gln14 or Gln20 of CT, the corresponding GlcNAc bearing peptide was prepared using *N*-acetyl-D-glucosaminyl-L-glutamine (Gln(GlcNAc)) as a building block [29], in which the reducing end of the GlcNAc residue was bound to the N atom of the side chain amide of Gln residue in a β-anomeric configuration, similar to Asn(GlcNAc). When CT14-GlcNAc was used as a glycoside acceptor, the transglycosylation to Gln(GlcNAc) [30] proceeded as efficiently as that to Asn(GlcNAc) (Figure 1c).

Table 1. List of N-glycosylated CT derivatives prepared

Name	*Glycosylation site*	*Structure of oligosaccharide*
CT		(none)
CT3-GlcNAc	Asn3	GlcNAc
CT3-STF	Asn3	(NeuAc-Gal-GlcNAc-Man)$_2$-Man-GlcNAc$_2$
CT3-ASTF	Asn3	(Gal-GlcNAc-Man)$_2$-Man-GlcNAc$_2$
CT3-dGal	Asn3	(GlcNAc-Man)$_2$-Man-GlcNAc$_2$
CT3-Core	Asn3	Man$_3$-GlcNAc$_2$
CT3-M_1GN_2	Asn3	Man-GlcNAc$_2$
CT3-GN_2	Asn3	GlcNAc$_2$
CT14-GlcNAc	Gln14	GlcNAc
CT14-STF	Gln14	(NeuAc-Gal-GlcNAc-Man)$_2$-Man-GlcNAc$_2$
CT14-ASTF	Gln14	(Gal-GlcNAc-Man)$_2$-Man-GlcNAc$_2$
CT20-GlcNAc	Gln20	GlcNAc
CT20-STF	Gln20	(NeuAc-Gal-GlcNAc-Man)$_2$-Man-GlcNAc$_2$
CT20-ASTF	Gln20	(Gal-GlcNAc-Man)$_2$-Man-GlcNAc$_2$
[Asn^{26}]-CT		(none)
CT26-GlcNAc	Asn26	GlcNAc
CT26-STF	Asn26	(NeuAc-Gal-GlcNAc-Man)$_2$-Man-GlcNAc$_2$
CT26-ASTF	Asn26	(Gal-GlcNAc-Man)$_2$-Man-GlcNAc$_2$

*Amino acid sequence of eel calcitonin: CysSerAsn^{3}LeuSerThrCysValLeuGlyLysLeuSerGln^{14}GluLeuHisLysLeuGln^{20}ThrTyrProArgTheAsp^{26}Val-GlyAlaGlyThrPro-NH_2.

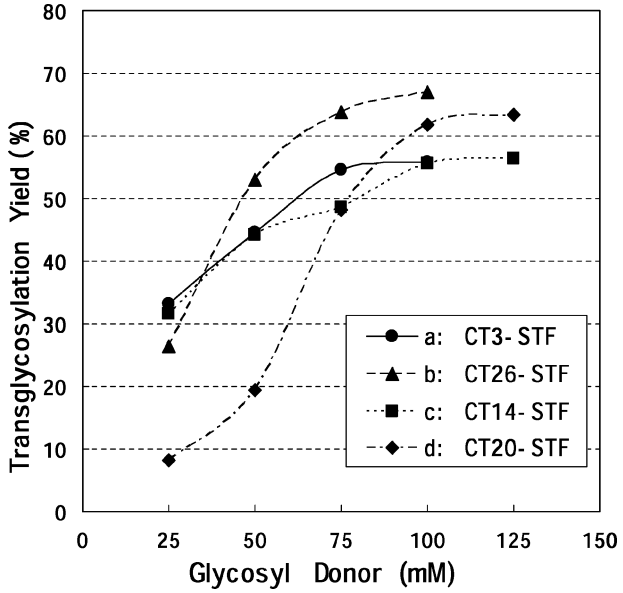

Figure 1. Effect of glycosyl donor concentration on the transglycosylation of CT-GlcNAc derivatives catalyzed by Endo-M. The reaction mixture consisted of 10 mM CT-GlcNAc derivative, 25 to 125 mM SGP, 120 mU/ml of Endo-M and 60 mM potassium phosphate buffer (pH 6.25), and was incubated at 37°C for 20 min. Acceptors are CT3-GlcNAc (●), CT26-GlcNAc (▲), CT14-GlcNAc (■) and CT20-GlcNAc (♦).

The transglycosylation to CT20-GlcNAc also proceeded quite efficiently, although the SGP dose-dependency of the transglycosylation to CT20-GlcNAc was somewhat different from that of the other derivatives (Figure 1d).

The CT derivatives possessing asialo complex-type oligosaccharides, CT3-ASTF, CT14-ASTF, CT20-ASTF and CT26-ASTF, were prepared in good yield by treatment of CT3-STF, CT14-STF, CT20-STF and CT26-STF, respectively, with neuraminidase.

CT derivatives containing various lengths of oligosaccharides attached to Asn3 were prepared from CT3-STF by the step-wise cleavage of the non-reducing terminal glycoside moieties using several exo-glycosidases. β-Galactosidase treatment of CT3-ASTF gave CT3-dGal. β-*N*-Acetylhexosaminidase treatment of CT3-dGal gave CT3-Core. The α1-2,3,6-mannosidase treatment of CT3-Core gave CT3-M_1GN_2. The β-mannosidase treatment of CT3-M_1GN_2 gave CT3-GN_2. All the trimming reactions were quite efficient.

Effect of N-linked oligosaccharide on the three-dimensional structure

All of the N-glycosylated CT derivatives synthesized in this study showed CD spectra that were quite similar to that of CT, irrespective of the site of attachment or the structure of the oligosaccharide. The structural stability of these CT derivatives was also examined by increasing the temperature used in the CD measurements. Although the helical content in an aqueous solution of 40% TFE decreased proportional to the temperature increase, no remarkable difference in the slope was observed for CT or any of the glycosylated derivatives (data not shown).

We observed a small reduction in the helical content for CT20-STF and CT20-ASTF, although almost no change in the helical content of CT20-GlcNAc was detected. Since the

Table 2. Hypocalcemic activity and receptor binding activity of N-glycosylated eel calcitonin derivatives

N-glycosylated CT derivatives	*Hypocalcemic activity (%)**	*Receptor binding activity (%)**
CT	100	100
CT3-GlcNAc	114	86
CT3-STF	97	6
CT3-ASTF	101	21
CT3-dGal	116	39
CT3-Core	125	54
CT3-M_1GN_2	144	53
CT3-GN_2	130	78
CT14-GlcNAc	110	58
CT14-STF	91	3
CT14-ASTF	115	16
CT20-GlcNAc	157	86
CT20-STF	170	46
CT20-ASTF	169	66
[Asn^{26}]-CT	104	187
CT26-GlcNAc	111	214
CT26-STF	186	66
CT26-ASTF	175	107

*Hypocalcemic activity and receptor binding activity are expressed as the relative value to that of CT. Standard deviation of hypocalcemic activity and 95% confidence limit of receptor binding activity are summarized in Materials and methods.

change was small and the carbohydrate moiety might have affected the determination of concentration by the HPLC peak area at 210 nm, this structural change cannot be considered to be conclusive. Studies of the structures of these glycopeptides by NMR are currently underway.

Effect of N-linked oligosaccharide on hypocalcemic activity

The hypocalcemic activity of CT derivatives in which the Asn or Gln residues were N-glycosylated was not substantially different from that of CT, as shown in the relative activity values to that of CT in Table 2 (second column). When the Asn3 residue was N-glycosylated with disialo or asialo complex-type oligosaccharides, the activity remained essentially unchanged. The N-glycosylated CT derivatives at the Gln14 residue showed an activity similar to that of CT. N-glycosylation of the Gln20 residue with GlcNAc or disialo and asialo complex-type oligosaccharides resulted in an enhanced activity. Neither the replacement of Asp26 to Asn26 nor GlcNAc attachment at this position affected the activity to any extent. N-glycosylation of the Asn26 residue with disialo or asialo complex-type oligosaccharides, however, significantly enhanced the hypocalcemic activity. Thus, N-glycosylated CT exhibited different effects depending on the site of attachment and the type of oligosaccharide attached. It is noteworthy that a stronger activity enhancement was observed for 20th and 26th position than for 3rd and 14th position, indicating that the change in activity is not dependent on the amino acid residue.

Effect of N-linked oligosaccharide on receptor binding activity

The receptor binding activity of the CT derivatives was measured using a direct competition assay using mouse osteoclast-like cells and ^{125}I-labelled elcatonin, a synthetic analogue of eel CT having CT receptor (CT-R) binding activity and hypocalcemic activity comparable to eel CT [11]. From the IC_{50} values for the competition of CT or the glycosylated CT derivatives with ^{125}I-elcatonin binding to CT-R on the osteoclast-like cells, the binding activity of the N-glycosylated CT derivatives relative to that of CT was calculated, and these data are shown in Table 2 (third column). A general trend for the larger oligosaccharide to have a smaller binding activity was found. Among these, CT3-STF and CT14-STF had a dramatically decreased binding activity of less than one tenth that of CT. [Asn^{26}]-CT and CT26-GlcNAc showed the highest binding activity of about twice the activity of CT.

Effect of N-linked oligosaccharide on biodistribution

Using radioisotope-labelled CT derivatives, in which the Tyr22 residue was labelled with ^{125}I, their distribution was studied in mice. The distribution of CT3-STF, CT3-ASTF, [Asn^{26}]-CT, CT26-STF and CT26-ASTF in the blood, bone, liver and kidney is shown in Figure 2. All the samples followed similar time course in the blood concentration, but CT3-ASTF showed highest concentration and CT26-ASTF did the lowest. Although the error bars were large in the bone concentration, [Asn^{26}]-CT showed relatively high accumulation among them. The sialo CT derivatives accumulated to a greater extent in the kidney and less in the liver, and asialo CT derivatives accumulated to a lesser extent in the kidney and more in the liver. Although the same oligosaccharide structure had the same preference with respect to organs, the relative concentration and profile differed depending on the glycosylation site.

Discussion

To study the site-dependent effect of N-glycosylation, we chose Asp26, Gln14 and Gln20 as glycosylation sites in addition to Asn3 based on the structural and chemical similarity with Asn. Because the amino acid sequences around those three residues do not have any resemblance to the consensus sequence of N-glycosylation and a Gln residue differs from Asn by only one methylene group, one of the important issues in this study was whether the introduction of an N-linked oligosaccharide by Endo-M into those amino acid residues of CT was possible.

As disclosed in the Results section, a combination of a recombinant Endo-M and a large excess of glycosyl donor in the form of SGP gave good transglycosylation yields, reaching 60% or more. The transglycosylation of Gln(GlcNAc) proceeded with a efficiency similar to that of Asn(GlcNAc). Although a slight

positional effect was observed in the case of CT20-GlcNAc, the most important requirement of the transglycosylation reaction with Endo-M was shown to be the presence of a GlcNAc residue.

All the N-glycosylated CT derivatives synthesized in this study showed CD spectra that were quite similar to that of CT, indicating that the three-dimensional structure of the peptide backbone is not affected by N-glycosylation, irrespective of the carbohydrate structure or the glycosylation site. Also, all the N-glycosylated CT derivatives with complex-type oligosaccharides retained hypocalcemic activity, and the effect of N-glycosylation was shown rather mild. However, among the mild changes, the effect appeared to be dependent on both the glycosylation site and the carbohydrate structure. The change in hypocalcemic activity as the result of N-glycosylation at Asn3 or Gln14 was smaller than at Gln20 or Asp26. This result clearly shows that the effect of N-glycosylation is position-dependent and not amino acid-dependent.

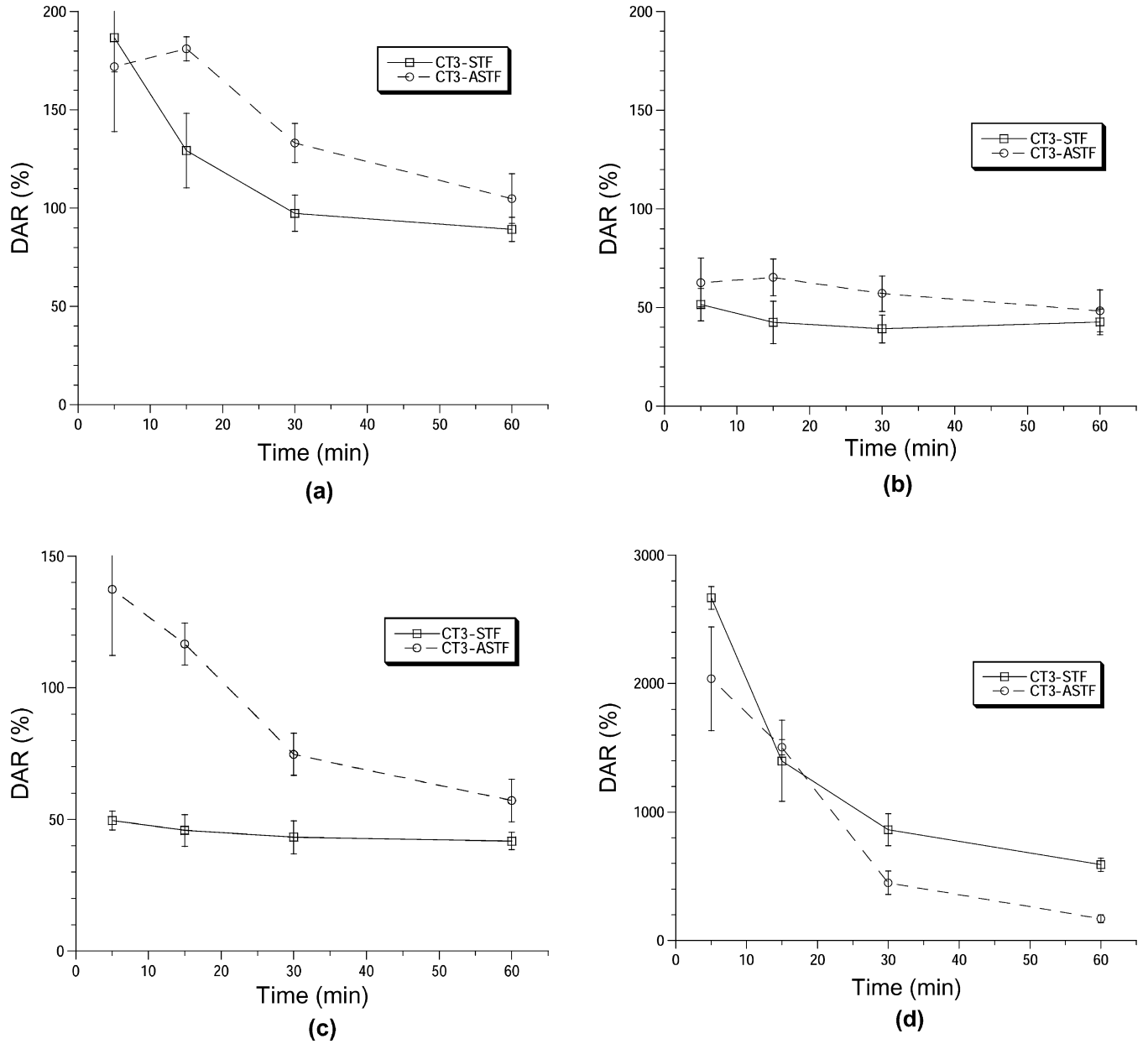

Figure 2. Biodistribution of N-glycosylated CT derivatives in the blood, bone, liver and kidney studied by injecting radioisotope-labeled compounds into mice. The biosistribution of CT3-STF(□) and CT3-ASTF (○) in blood (a), bone (b), liver (c) and kidney (d), and [Asn26]-CT (●), CT26-STF (□) and CT26-ASTF (○) in blood (e), bone (f), liver (g) and kidney (h) is shown.

(*Continued on next page.*)

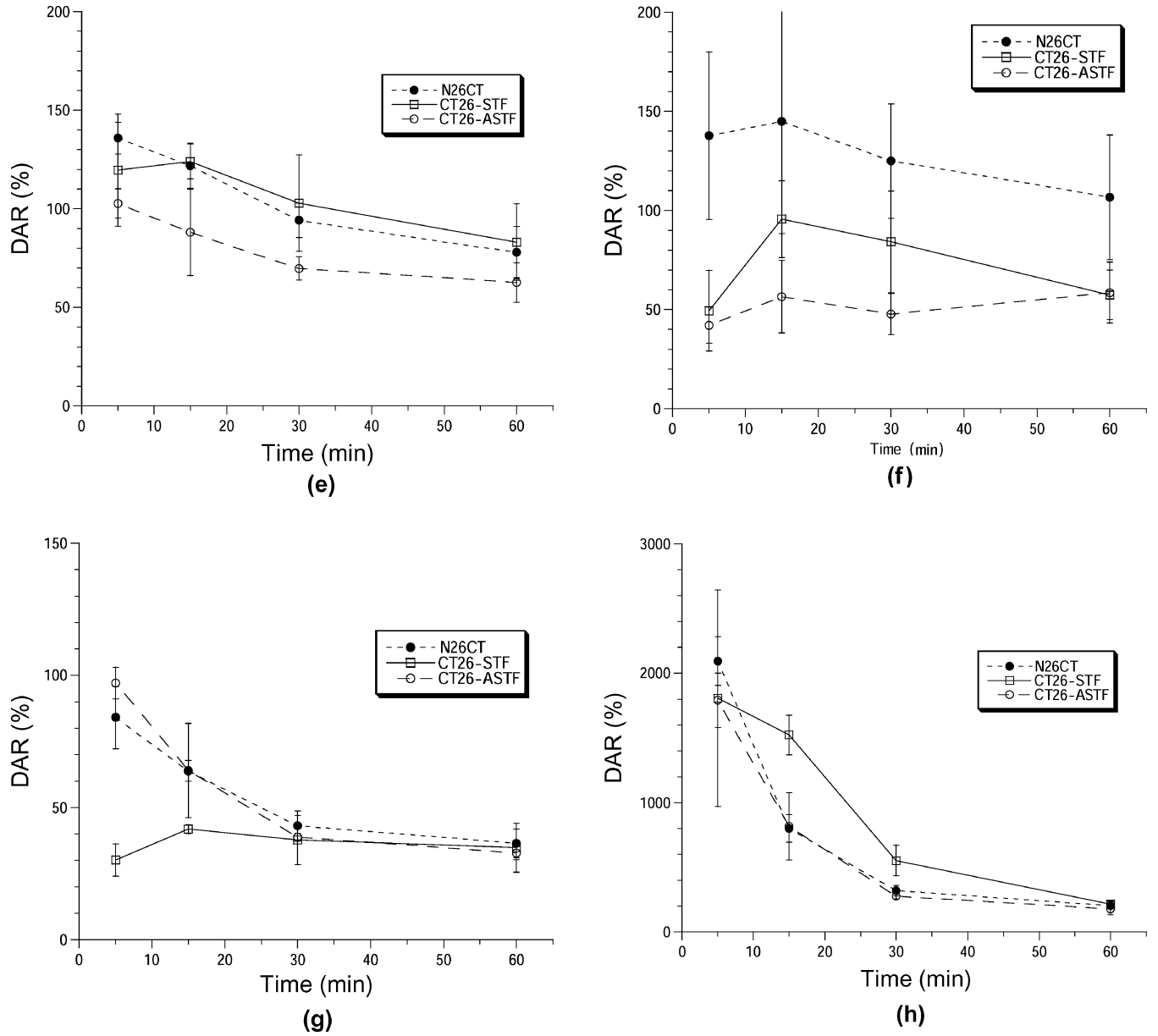

Figure 2. (*Continued*).

It has been reported that the hypocalcemic activity of CT derivatives is primarily correlated with their receptor binding activity [6,9]. The introduction of complex-type oligosaccharides into any Asn, Asp or Gln site of CT led to a decrease in the receptor binding activity. There is a general trend that larger oligosaccharides have smaller binding activities, as clearly demonstrated in the truncation series of oligosaccharides at Asn3. The addition of GlcNAc had the smallest effect on binding activity. The introduction of GlcNAc to Asn26 greatly increased binding activity. Because the replacement of Asp26 with Asn enhanced CT-R binding activity, the effect of GlcNAc attachment at this site might reflect this amino acid substitution effect. The N-glycosylated CT derivatives at Gln20 and Asn26 showed relatively high CT-R binding activities, which may explain the high hypocalcemic activity of these derivatives. However, the binding data alone do not fully explain the hypocalcemic activity. The IC_{50} value of CT3-STF decreased to less than one tenth that of CT, even though it had a hypocalcemic activity similar to CT. The introduction of complex-type oligosaccharide to the Gln14 residue showed a similar contradiction between hypocalcemic activity and CT-R binding activity.

For a better understanding of the discrepancy between the hypocalcemic activity and the receptor binding activity, the biodistribution of CT derivatives in living organisms was studied. Because we employed different animals, rats

for hypocalcemic and mice for biodistribution experiments, we could not obtain quantitatively consistent results. The following discussion, however, can qualitatively explain the discrepancy.

Reflecting its high receptor binding activity, the concentration of [Asn^{26}]-CT was kept high in the bone where CT-R is abundantly expressed. From the biodistribution in the liver and kidney, it was shown that the STF derivatives escaped from the liver and ASTF derivatives escaped from the kidney. The asialoglycoprotein receptor (ASGP-R) in liver is a well-known galactose receptor [31], and it is reasonable that CT-ASTF would accumulate in the liver, resulting in lower levels in the kidney. On the contrary, CT-STF escapes liver accumulation and hence accumulates in relative abundance in the kidney which controls electrolyte balance.

The decrease in receptor binding activity of CT-STF may be compensated by this biodistribution, and may explain the fact that the hypocalcemic activity of CT-STF is not drastically decreased, or even enhanced in the case of CT20-STF and CT26-STF. This mechanism for activity enhancement is analogous to the effect of GlcNAc attachment in that glycosylation reduces the liver trap, but the effect seems to be much greater in the case of STF attachment.

However, the biodistribution study poses another paradox. Why does CT-ASTF exhibit a high hypocalcemic activity in spite of its accumulation in the liver? To answer this paradox, the fate of the CT derivative after liver accumulation must be considered. Without glycosylation, CT enters the excretion pathway common to hydrophobic peptides [32]. With glycosylation, CT-ASTF is trapped by ASGP-R, but the ASGP-R related pathway permits the release and recirculation of the trapped glycopeptide [33,34]. Because the recirculation pathway prevents a part of the liver metabolism, CT-ASTF is able to retain the hypocalcemic activity level of CT. This effect is reflected in the relatively high blood concentration of CT3-ASTF. The difference between CT3-ASTF and CT26-ASTF in the liver accumulation may correspond to their relative concentration in the blood.

Thus, carbohydrates show quite different functions depending on their structure, even though the apparent hypocalcemic activities are similar. The STF carbohydrate induces more hindrance in receptor binding than ASTF. Although reduced receptor binding generally results in reduced hypocalcemic activity, CT-STF and CT-ASTF retain their hypocalcemic activities due at least in part to their altered biodistribution, even though their organ preferences are quite different.

In conclusion, the use of an excess of a SGP glycosyl donor and a recombinant Endo-M gave a good yield in the transglycosylation of a complex-type oligosaccharide from a glycosyl donor to the GlcNAc residue of CT derivatives irrespective of the glycosylation site and whether the residue was Asn or Gln. The synthesized compounds revealed the structural and the positional effects of N-glycosylation. Although the change was milder than the effect of O-glycosylation, both the carbohydrate structure and the position of glycosylation affected the biological activities of CT without any significant change in three-dimensional structure.

Acknowledgments

This work was supported, in part, by Grant-in Aids for Scientific Research (No. 11650825) from the Ministry of Education, Science, and Culture of Japan and the Research and Development Projects of Industrial Science and Technology Frontier Program supported by NEDO (New Energy and Industrial Technology Development Organization). We thank Prof. K. Kuwajima and Dr. M. Arai of the University of Tokyo for their helpful advice and use of a CD spectrometer. The hypocalcemic activity was measured at the Toyo Kensa Center.

References

1 Varki A, Biological roles of oligosaccharides: All of the theories are correct, *Glycobiology* **3**, 97–130 (1993).
2 Dwek RA, Toward understanding the function of sugars, *Chem Rev* **96**, 683–720 (1996).
3 Rudd RM, Joao HC, Coghill E, Fiten P, Saunders MR, Opdenakker G, Dwek RA, Glycoforms modify the dynamic stability and functional activity of an enzyme, *Biochemistry* **33**, 17–22 (1994).
4 Blithe DL, Biological functions of oligosaccharides on glycoproteins, *Trends Glycosci Glycotech* **5**, 81–98 (1993).
5 Hashimoto H, Toma K, Nishikido J, Yamamoto K, Haneda K, Inazu T, Valentine KG, Opella SJ, Effects of glycosylation on the structure and dynamics of eel calcitonin in micelles and lipid bilayers determined by nuclear magnetic resonance spectroscopy, *Biochemistry* **38**, 8377–84 (1999).
6 Tagashira M, Tanaka A, Hisatani K, Isogai Y, Hori M, Takamatsu S, Fujibayashi Y, Yamamoto K, Haneda K, Inazu T, Toma K, Effect of carbohydrate structure on biological activity of artificially N-glycosylated eel calcitonin, *Glycoconjugate J* **18**, 449–55 (2001).
7 Tagashira M, Iijima H, Isogai Y, Hori M, Takamatsu S, Fujibayashi Y, Haneda K, Inazu T, Toma K, Site-independent activity enhancement of calcitonin by *N*-acetylglucosamine attachment. In *Peptide Science 2000*, edited by Shimonishi T (Protein Research Foundation, Osaka, 2001), pp. 125–8.
8 Tagashira M, Iijima H, Toma K, Three-dimensional structure and biological activity of glycosylated calcitonin, *Trends Glycosci Glycotech* **13**, 373–83 (2001).
9 Tagashira M, Iijima H, Isogai Y, Hori M, Takamatsu S, Fujibayashi Y, Yoshizawa-Kumagaye K, Isaka S, Nakajima K, Yamamoto T, Teshima T, Toma K, Site-dependent effect of O-glycosylation on the conformation and biological activity of calcitonin, *Biochemistry* **40**, 11090–5 (2001).
10 Tagashira M, Iijima H, Toma K, An NMR study of O-glycosylation induced structural changes in the α-helix of calcitonin, *Glycoconjugate J* **19**, 43–52 (2002).
11 Azria M, *The Calcitonins: Physiology and Pharmacology* (Karger, Basel, 1989).
12 Inazu T, Kobayashi K, A new simple method for the synthesis of N^{α}-Fmoc-N^{β}-glycosylated-L-asparagine derivative, *Synlett* 869–70 (1993).

13 Inazu T, Kobayashi K, Yaginuma H, A new synthetic method for N$^{\beta}$-glycosylated-L-asparagine derivatives, and the solid-phase synthesis of N-glycopeptides. In *Peptide Chemistry 1993*, edited by Okada Y (Protein Research Foundation, Osaka, 1994), pp. 101–4.
14 Haneda K, Inazu T, Yamamoto K, Kumagai H, Nakahara Y, Kobata A, Transglycosylation of intact sialo complex-type oligosaccharides to the *N*-acetylglucosamine moieties of glycopeptides by *Mucor hiemalis* endo-β-*N*-acetylglucosaminidase, *Carbohydr Res* **292**, 61–70 (1996).
15 Haneda K, Inazu T, Mizuno M, Yamamoto K, Chemoenzymatic synthesis of neoglycopeptide using endo-β-*N*-acetylglucosaminidase from *Mucor hiemalis*. In *Methods in Enzymology 362*, edited by Lee YC, Lee RC (Academic Press, Oxford, 2003), pp. 74–85.
16 Yamamoto Y, Kadowaki S, Watanabe J, Kumagai K, Transglycosylation activity of *Mucor hiemalis* endo-β-*N*-acetylglucosaminidase which transfers complex oligosaccharides to the *N*-acetylglucosamine moieties of peptides, *Biochem Biophys Res Commun* **203**, 244–52 (1994).
17 Haneda K, Inazu T, Mizuno M, Iguchi R, Yamamoto K, Kumagai H, Aimoto S, Suzuki H, Noda T, Chemo-enzymatic synthesis of calcitonin derivatives containing N-linked oligosaccharides, *Bioorg Med Chem Lett* **8**, 1303–6 (1998).
18 Mizuno M, Haneda K, Iguchi R, Muramoto I, Kawakami T, Aimoto S, Yamamoto K, Inazu T, Synthesis of a glycopeptide containing oligosaccharides: Chemoenzymatic synthesis of eel calcitonin analogues having natural N-linked oligosaccharides, *J Am Chem Soc* **121**, 284–90 (1999).
19 Yamamoto K, Haneda K, Iguchi R, Inazu T, Mizuno M, Takegawa K, Kondo A, Kato I, Chemo-enzymatic synthesis of a calcitonin derivative containing a high-mannose type oligosaccharide by endo-β-*N*-acetylglucosaminidase from *Arthrobacter protophormiae*, *J Biosci Bioeng* **87**, 175–9 (1998).
20 Mizuno M, Recent trends in glycopeptide synthesis, *Trends Glycosci Glycotech* **13**, 11–30 (2001).
21 O'Connor SE, Pohlmann J, Imperiali B, Saskiawan I, Yamamoto K, Probing the effect of the outer saccharide residues of N-linked glycans on peptide conformation, *J Am Chem Soc* **123**, 6187–8 (2001).
22 Ajisaka A, Miyasato M, Ito C, Fujita Y, Yamazaki Y, Oka S, Linkage of sugar chains to a fragment peptide of FGF-5S by a chemoenzymatic strategy and changes in the rate of proteolytic hydrolysis, *Glycocojugate J* **18**, 301–8 (2001).
23 Kobayashi K, Takeuchi M, Iwamatsu A, Yamamoto K, Kumagai H, Yoshida S, *JP* 11332568 (1999).
24 Seko A, Koketsu M, Nishizono M, Enoki Y, Ibrahim HR, Juneja LR, Kim M, Yamamoto T, Occurrence of a sialylglycopeptide and free sialylglycans in hen's egg yolk, *Biochim Biophys Acta* **1335**, 23–32 (1997).
25 Chen YH, Yang JT, Martinez HM, Determination of the secondary structure of proteins by circular dichroism and optical rotatory dispersion, *Biochemistry* **11**, 4120–31 (1972).
26 Otani M, Kitazawa S, Yamauchi H, Meguro T, Orimo H, Stability and the biological activity of eel calcitonin in rats, *Horm Metab Res* **10**, 252–6 (1978).
27 Akatsu T, Tamura T, Takahashi N, Udagawa N, Tanaka S, Sasaki T, Yamaguchi A, Nagata N, Suda T, Preparation and characterization of a mouse osteoclast-like multinucleated cell population, *J Bone Mineral Res* **7**, 1297–306 (1992).
28 Tamura T, Takahashi N, Akatsu T, Sasaki T, Udagawa N, Tanaka S, Suda T, New resorption assay with mouse osteoclast-like multinucleated cells formed *in vitro*, *J Bone Mineral Res* **8**, 953–60 (1993).
29 Mizuno M, Muramoto I, Kobayashi K, Yaginuma H, Inazu T, A simple method for the synthesis of N$^{\beta}$-glycosylated-asparagine and -glutamine derivatives, *Synthesis* 162–5 (1999).
30 Haneda K, Inazu T, Mizuno M, Iguchi R, Tanabe H, Fujimori K, Yamamoto K, Kumagai H, Tsumori K, Munekata E, Chemoenzymatic synthesis of a bioactive peptide containing a glutamine-linked oligosaccharide and its characterization, *Biochim Biophys Acta* **1526**, 242–8 (2001).
31 Hudgin RL, Pricer WE, Jr, Ashwell G, Stockert RJ, Morell AG, The isolation and properties of a rabbit liver binding protein specific for asialoglycoprotein, *J Biol Chem* **249**, 5536–43 (1974).
32 Ruwart MJ, Approaches to modulating liver transport of peptide drugs. In *Peptide-Based Drug Design*, edited by Taylor MD, Amidon GL (American Chemical Society, Washington, DC, 1995), pp. 249–62.
33 Connolly DT, Townsend RR, Kawaguchi K, Bell WR, Lee YC, Binding and endocytosis of cluster glycosides by rabbit hepatocytes, *J Biol Chem* **257**, 939–45 (1982).
34 Regoeczi E, Chindemi PA, Debanne MT, Hatton MWC, Dual nature of the hepatic lectin pathway for human asialotransferrin type 3 in the rat, *J Biol Chem* **257**, 5431–6 (1982).

Received 11 February 2004; revised 9 June 2004;
accepted 7 July 2004